Article

Not peer-reviewed version

Entropy and Energy for Non-Mechanical Work at the Bose-Einstein Transition of a Harmonically Trapped Gas Using an Empirical Global-Variable Method

Marcos Miotti *, Edmur Braga Martins, Michał Hemmerling, Romain Dubessy, Vanderlei Salvador Bagnato

Posted Date: 18 June 2024

doi: 10.20944/preprints202406.1225.v1

Keywords: Entropy; Bose-Einstein Condensation; Quantum Thermal Engines; Quantum Gases

Article

Entropy and Energy for Non-Mechanical Work at the Bose-Einstein Transition of a Harmonically Trapped Gas Using an Empirical Global-Variable Method

Marcos Miotti[1,†,*], Edmur Braga Martins[1,†], Michał Hemmerling[1], Romain Dubessy[2], Vanderlei Salvador Bagnato[1,3]

[1] São Carlos Institute of Physics, University of São Paulo, São Carlos, Brazil, PO Box 369
[2] Laboratoire de Physique des Lasers, Université Sorbonne Paris Nord, CNRS UMR 7538, F-93430 Villetaneuse, France [3] Biomedical Engineering Department, Texas A&M University, College Station, TX 77843, USA
* Correspondence: marcos.miotti@alumni.usp.br
† These authors contributed equally to this work.

Abstract: Quantum thermal engines are receiving much attention in recent years, due to their potential applications. For a candidate group, harmonically trapped gases under Bose-Einstein condensation (BEC), we see little investigation on the energy transference around that transition. Therefore, we present an empirical study with rubidium-87 gas samples in a magnetic harmonic trap. We developed an empirical Equation of State model to fit to our experimental dataset, expressing the pressure parameter ($\mathcal{P}$) in terms of temperature (T) and six technical coeffcients ($\{a_i\}_{0,\dots,4}$, T_{th}), functions of volume parameter ($\mathcal{V}$) and number of atoms (N). For weakly interacting gases, the internal energy is $U \cong 3\mathcal{P}\mathcal{V}$, thus we determine the entropy with $U = TS - \mathcal{P}\mathcal{V}$ for fixed N. As expected, we show that the entropy at the BEC transition (S_c) is constant for varying $\mathcal{V}$. Being isentropic makes BEC transition an energy source for non-mechanical work. Hence, we observed that the enthalpy at the BEC transition $H_c = E_c + \mathcal{P}_c\mathcal{V} = T_c S_c$, at fixed values of $\mathcal{V}$ and varying N, grows fairly linearly with N. We fitted $H_c = \eta N - H_c^0$ to that data, being η the specific enthalpy of BEC transformation and H_c^0 an intrinsic enthalpic loss. We deem this study to be a step closer to practical quantum-based engines.

Keywords: Entropy, Bose-Einstein Condensation, Quantum Gases, Quantum Thermal Engines

1. Introduction

With the discussions in mainstream media and the nearing deployment of operational quantum computers and other quantum-based technologies for actual applications, some branches of contemporary research on quantum thermodynamics have been devoted towards that goal, as classical thermodynamics was one of the major technoscientific causes for the First Industrial Revolution. In particular, the development of the so-called *quantum thermal engines* [1], which are machines running on thermal energy sources at microscopic scale, has been a topic of interest in recent years. When it comes to thermal engines in classical thermodynamics, it is natural to think of devices using gases for combustion or work generation. To the latter, ultracold, quantum-degenerated gases seem promising candidates for building real quantum thermal engines. Indeed, Sur and Ghosh [2] have recently pointed out the advantages of using Fermi and Bose gases in quantum engines. Koch and co-workers [3] have actually implemented a thermal engine operating at the BEC-BSC crossover, showing that a phase transition in a bosonic-fermionic system is a viable energy source for work. In the particular case of bosonic systems, Eglinton and co-workers [4] have indicated a performance boost for a quantum engine running on a gas under Bose-Einstein condensation (BEC) under certain configurations. In the current year, Estrada and co-workers [5] analyzed theoretically the role of interactions in the efficiency of thermal engine running on a harmonically confined gas under BEC. However, after reviewing the recent literature, we believe that the field of weakly interacting gases under BEC in a harmonic potential still lacks an experimental investigation of thermodynamic properties

Citation: Miotti, M.; Martins, E. B. et al. Entropy and Energy for Non-Mechanical Work at the Bose-Einstein Transition of a Harmonically Trapped Gas Using an Empirical Global-Variable Method. *Entropy* **2024**, *1*, 0. https://doi.org/

Received:
Revised:
Accepted:
Published:

 doi:10.20944/preprints202406.1225.v1

at the BEC transition pinpointing their use for building quantum thermal engines, which we hope to address in this paper.

In the last year [6], we demonstrated theoretically and experimentally that the efficiency of Carnot cycles is always $1 - T_{\mathrm{cold}}/T_{\mathrm{hot}}$ before, across and after BEC, therefore showing that result to hold true in both classical and quantum regimes, as well as in the transition between them. For that end, we have used experimental data and the methodology firstly described on the corresponding author's Master thesis [7], which relied on a formalism called Global-Variable Method [8–10], an approach parallel to Local Density Approximation [11] in describing the thermodynamics of inhomogeneous quantum gases (remarkably, the harmonically trapped ones). Now, using the same data and approach, we present here a strictly experimental investigation on the BEC transition as a energy source for non-mechanical work, a topic is seldomly explored in literature. Although more modern techniques are already available for producing gas samples under BEC at constant density in box-like potentials [12], making thermodynamic analysis much easier, the simplicity and reliability of over fourty years of expertise [13] on harmonically trapping ultracold gases and the existence of operating BEC laboratories with harmonic-trap setups justify using the Global-Variable Method, as that mathematical formalism itself is already available.

The remainder of this paper is organized as follows: in Sec. 2, we review the Global-Variable Method, which was used for determining the thermodynamic quantities in our experiments; in Sec. 3, we describe briefly our apparatus for producing gases under BEC and the techniques used in our experiments; in Sec. 4, we present a full thermodynamic description of harmonically trapped gas samples across BEC, showing that entropy is constant at the phase transition and investigating the energy available for non-mechanical work at it; in Sec. 5, we map out the steps for designing a quantum thermal engine running on a harmonically trapped gas based on Secs. 3 and 4, and in Sec. 6, we wrap up the results and their discussions in this paper.

2. Global-Variable Method

Differently from an ideal gas in a box-like potential, for which the confining volume (V) in space is well-defined, an ideal gas in a harmonic potential $U_{\mathrm{h}}(\boldsymbol{r}) = (m/2)(\omega_x^2 x^2 + \omega_y^2 y^2 + \omega_z^2 z^2)$ covers the whole space theoretically, which means that neither its volume nor its pressure (which forms a conjugate pair with volume) are well-defined. However, it is still possible to find thermodynamic quantities for that kind of system, being one of few analytically solvable quantum many-body problems out there. By the using the Bose-Einstein statistics in limit that the energy level spacing is much lower than the thermal energy kT, being T the temperature, the total number of atoms and the internal energy of an ideal gas in a harmonic potential are described as

$$N(T,\bar{\omega}) = \left(\frac{kT}{\hbar\bar{\omega}}\right)^3 g_3(e^{\mu/(kT)}) \tag{1}$$

$$\text{and} \qquad U(T,\bar{\omega}) = 3kT\left(\frac{kT}{\hbar\bar{\omega}}\right)^3 g_4(e^{\mu/(kT)}) \tag{2}$$

respectively, in which $\bar{\omega} = (\omega_x\omega_y\omega_z)^{1/3}$, μ is the chemical potential and $g_\nu(\xi) = \sum_{i=1}^{\infty} \xi^i/i^\nu$ is the polylogarithm (usually called "Bose function" among physicists). By making $\mu = 0$, one of the conditions for BEC in ideal gases, we find the *critical temperature* for that phenomenon to happen from Eq. (1):

$$T_c(N,\bar{\omega}) = \frac{\hbar\omega}{k}\left(\frac{N}{g_3(1)}\right)^{1/3} \tag{3}$$

Being N and U both extensive quantities, it means that some quantity on the right-hand side of Eqs. (1) and (2) must also be extensive, and it is $\bar{\omega}$ – which is logical, as the squared frequencies of a harmonic potential are directly proportional to how confining it is in each direction. On that account, let us define the quantity

 doi:10.20944/preprints202406.1225.v1

$$\mathcal{V} \equiv 1/\bar{\omega}^3, \tag{4}$$

and substitute it into Eq. (3) to find

$$T_c(N,\mathcal{V}) = \frac{1}{[g_3(1)]^{1/3}}\frac{\hbar}{k}\left(\frac{N}{\mathcal{V}}\right)^{1/3}. \tag{5}$$

As the critical temperature is a universal property, Eq. (5) must hold in the thermodynamic limit ($N \to \infty$ and $V \to \infty$, thus $n = N/V =$ constant), which is equivalent to weaken the harmonic potential into all direction, releasing atoms as their number grow. In that way, $\bar{\omega} \to 0$, which from Eq. (4) makes $\mathcal{V} \to \infty$ as $N \to \infty$, hence $N/\mathcal{V} =$ constant in the thermodynamic limit, with Eq. (5) holding true.

For its extensivity and analogy with volume, $\mathcal{V}$ defined in Eq. (4) is called *volume parameter*. Indeed, Romero and Bagnato [8–10] demonstrated together that $\mathcal{V}$ forms a conjugate pair with a quantity appropriately called *pressure parameter*, defined as

$$\mathcal{P} = \frac{2}{3\mathcal{V}}\int\limits_{V(U_\mathrm{h})} n(\boldsymbol{r})U_\mathrm{h}(\boldsymbol{r})\,\mathrm{d}^3r, \tag{6}$$

in which n is the spatially distribuited atomic density of the gas trapped by the harmonic potential U_h. That quantity is shown to be analogous to the hydrostatisc pressure of a thermalized fluid at rest within a harmonic potential. Hence, having the conjugate variables of mechanical work, it is possible to give a full thermodynamic description of a harmonically trapped gas. Our methods for implementing a harmonic trap for gas samples and measuring their density profiles is described in Sec. 3.

3. Thermodynamic Experiments

Our experimental setup for producing rubidium-87 (^{87}Rb) gas samples under BEC is the well-known double magneto-optical trap (MOT) system, whose construction and operation are detailed in Chapter 4 of Ref. [7]. In summary, hot ^{87}Rb gas is initially collected at the first MOT and transferred to the second MOT, in which the gas is cooled to millikelvins. The laser field is turned off once the second MOT is fully loaded, with atoms becoming confined in a purely magnetic trap, whose field is a "cigar-shaped" harmonic potential ($\omega_x \neq \omega_y = \omega_z$) with a non-zero mininum, ensuring the sample to be in a single hyperfine state (always $|F = 1, m_F = 2\rangle$ in our case). From there, the sample is subjected to submicrokelvin cooling by radiofrequency evaporation, finally reaching the temperature-density conditions for BEC.

Once the gas sample (commonly called *atomic cloud* or just *cloud*) at a steady, constant temperature state is prepared *in situ* the harmonic trap (whose frequencies are fixed, thus $\mathcal{V}$ from Eq. (4) is constant), its density is so high that it must be released from its confinement to freely expand adiabatically and isothermally before being imaged, a process known as *time-of-flight technique* (TOF), which destroys the sample. The cross section imaging of the gas sample allow us to determine its total number of atoms (N), *in situ* temperature (T) and expanded density profile n_TOF. To recover the *in situ* density profile (n) from n_TOF, we use the procedures of Castin-Dum regression [14] for the Bose-condensed fraction of atoms and You-Holland regression [15] for non-Bose-condesed (thermal) fraction of atoms. Having $\mathcal{V}$ and n, we determine the pressure parameter ($\mathcal{P}$) using Eq. (6). Therefore, we have the four required quantities (N, T, $\mathcal{V}$ and $\mathcal{P}$) to describe the thermodynamics of the system, as we discuss in Sec. 4. We recapitulate the contents on this section in Sec. 5.

4. Findings

After several months in laboratory, we have gathered a significantly large dataset of thermodynamic data, with twenty different values of N (ranging from 3.0×10^5 to 5.5×10^5 atoms), nineteen different values of $\mathcal{V}$ (ranging from 5.7×10^{-9} s^3 to 9.7×10^{-9} s^3), in the

 doi:10.20944/preprints202406.1225.v1

temperature range of $0.7T_c$ to $1.3T_c$. By fixing N and $\mathcal{V}$, the usual behavior of $\mathcal{P}$ versus T is seen in Fig. 1, which is the so-called *equation of state*.

From the overall behavior seen in Fig. 1, we designed an empirical expression for the equation of state, as stated in Eq. (7). For temperatures above the critical temperature (classical regime), any ideal gas is known to follow the Gay-Lussac's law, whose linear behavior is also seen in Fig. 1. Therefore, we used a generalized linear function (with the linear coefficient a_4 and the slope a_3) to fit to the data in the classical regime. For temperatures below the critical temperature (quantum regime), a harmonically confined ideal gas has an internal energy described by Eq. (2). Since $U \cong 3\mathcal{P}\mathcal{V}$ for both ideal and weakly interacting gases in a harmonic potential, we generalized the power-of-4 function to include a linear coefficient (a_2), an additional exponent (a_1) to temperature, and a different factor (a_0) multiplying temperature, fitting it to our data in the quantum regime. As the measurements of pressure parameter change smoothly between the quantum and classical regimes, the parameter we call *threshold temperature* (T_{th}) is defined at the point $\mathcal{P}_{T<T_c} = \mathcal{P}_{T>T_c}$. That temperature is lower the *actual* critical temperature, while being very close to its value.

$$\mathcal{P}(T,\mathcal{V},N) = \begin{cases} a_0(\mathcal{V},N)T^{4+a_1(\mathcal{V},N)} + a_2(\mathcal{V},N), & T < T_{\text{th}}(\mathcal{V},N);\ T_{\text{th}} \lesssim T_c. \\ a_3(\mathcal{V},N)T + a_4(\mathcal{V},N), & T > T_{\text{th}}(\mathcal{V},N). \end{cases} \tag{7}$$

From Eq. (7) and $U \cong 3\mathcal{P}\mathcal{V}$, we have a complete mapping of thermodynamics of a gas in a harmonic potential across the BEC transition. We demonstrate that by plotting $\mathcal{P} \times \mathcal{V}$ diagrams in Subsec. 4.1 and $T \times S$ diagrams in Subsec. 4.2. The latter will be particularly important in our analysis on the system's enthalpy in Subsec. 4.3. For a deeper inspection on the physical meanings of the technical coefficients in Eq. (7), check out Chapter 6 in Ref. [7].

 doi:10.20944/preprints202406.1225.v1

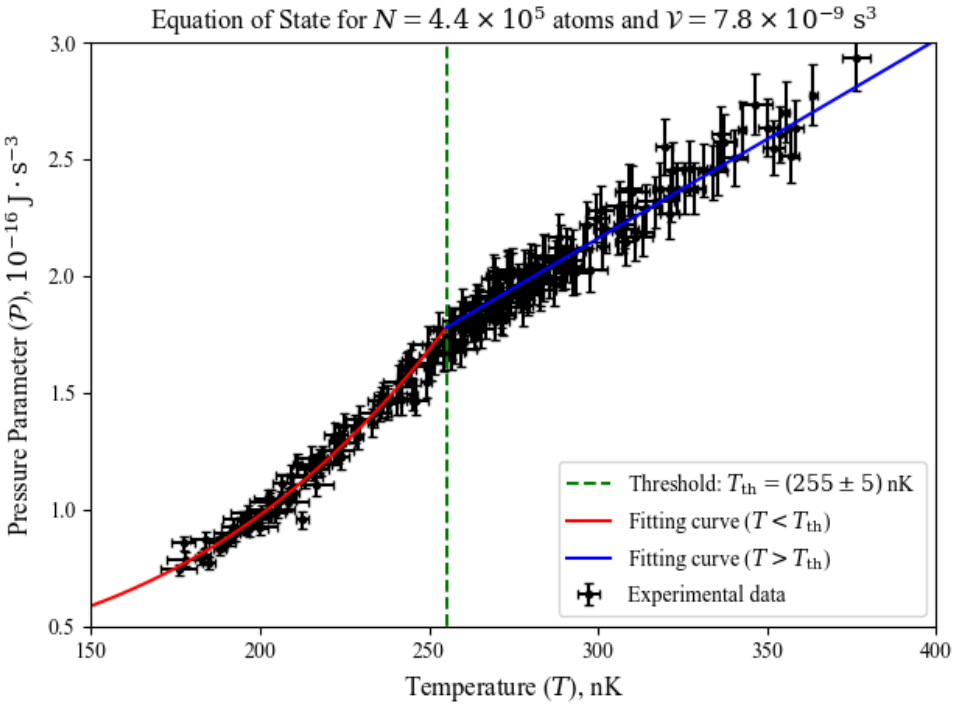

Figure 1. Behavior of the pressure parameter as a function of temperature across the BEC transition. The system smoothly transit from a linear behaior (the well-known Gay-Lussac's equation for classical gases) to a strongly nonlinear behavior (already indicated by Eq. (2)) as temperature decreases. The blue, red and green lines represent the components of our empirical model for the equation of state, seen in Eq. (7).

4.1. $\mathcal{P} \times \mathcal{V}$ Diagrams and the BEC Transition

To illustrate the BEC transition in a clear manner, we plotted four $\mathcal{P} \times \mathcal{V}$ diagrams at constant N in Fig. 2. The black curve represents how the BEC transition behaves as $\mathcal{V}$ varies from one experiment set to another. Above the black curves, the gas samples are purely thermal or classical, well described by the Maxwellian distribution of energy states. Below the black curves, the gas samples have suffered BEC, with a fraction of the atoms populating the ground state of the harmonic trap, whereas the rest, called thermal atoms, are still described by the Maxwellian distribution.

As a reminder of Ref. 3, the measurements have been done by fixing the volume parameter of the harmonic trap (i. e. characterizing its frequencies) and collecting data for various temperatures and number of atoms. In our experimental setup, before moving to a different volume parameter (by changing the current in the coils that generate the magnetic field for the second MOT and the magnetic trap). In our experimental setup, we did not have the flexibility of reliably changing the volume parameter of the harmonic trap without destroying the gas sample in that process. Althought challeging, that procedure is indeed possible, as we will discuss later on in Sec. 5. The fact of volume parameter being always constant in our measurements (i. e. no mechanical work is allowed in the system) influences our course of action in Subsecs. 4.2 and 4.3.

 doi:10.20944/preprints202406.1225.v1

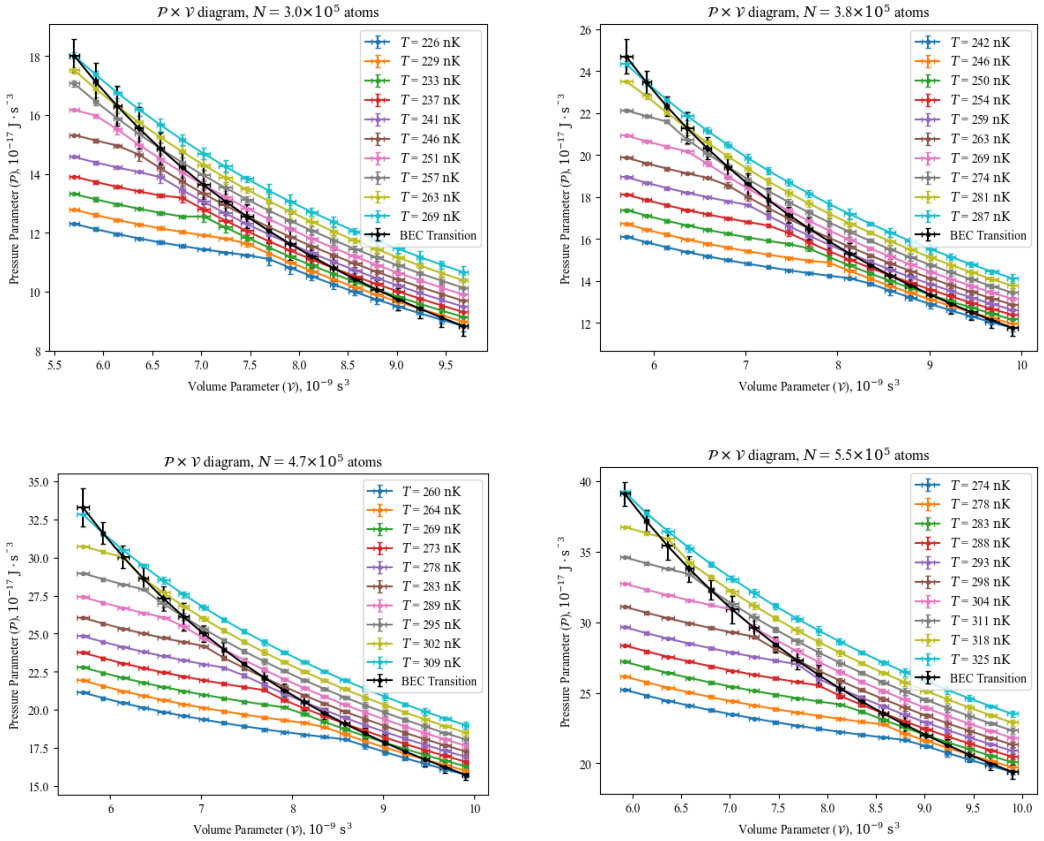

Figure 2. Selected pressure parameter ($\mathcal{P}$) versus volume parameter ($\mathcal{V}$) diagrams.

4.2. $T \times S$ Diagrams and the BEC Transition

As the expression for the internal energy of a weakly interacting Bose gas in a harmonic potential is well-known to be $U \cong 3\mathcal{P}\mathcal{V}$, we can use the relation $U = TS - \mathcal{P}\mathcal{V}$ for fixed values of N to find the *actual* entropy of the system. From Eq. (7), we get

$$S(T,\mathcal{V},N) = \begin{cases} 4\mathcal{V}[a_0(\mathcal{V},N)T^{3+a_1(\mathcal{V},N)} + a_2(\mathcal{V},N)/T], & T < T_{\text{th}}(\mathcal{V},N). \\ 4\mathcal{V}[a_3(\mathcal{V},N) + a_4(\mathcal{V},N)/T], & T > T_{\text{th}}(\mathcal{V},N). \end{cases} \tag{8}$$

whose plottings are shown in Fig. 3 for a four values of N. Notice that the points do not have error bars in the temperature axis, since T is an independent variable in both Eqs. (7) and (8), only used to generate the values and deviations for those equations of state. In the entropy axis, the magnitude of error bars are significantly larger than those in Fig. 2, due those error propagation in the operation $S = 4\mathcal{P}\mathcal{V}/T$, especially at the BEC transition (black curve), as the critical temperature T_c and model's threshold temperature T_{th} are both measured quantities, each having an associated error.

The black curves indicating the BEC transition in Fig. 3 are distinctive for having a constant entropy within the experimental error across the transition (which is significantly large due to error propagation in the entropy calculation), in agreement of the fact that BEC is not associated with any latent heat [16]. Since each individual gas sample in our experiments has been probed at constant values of $\mathcal{V}$, which prohibits mechanical work, we see that the BEC transition as a thermodynamic transformation could have been used as a source for non-mechanical work, as discussed in Sec. 4.3.

 doi:10.20944/preprints202406.1225.v1

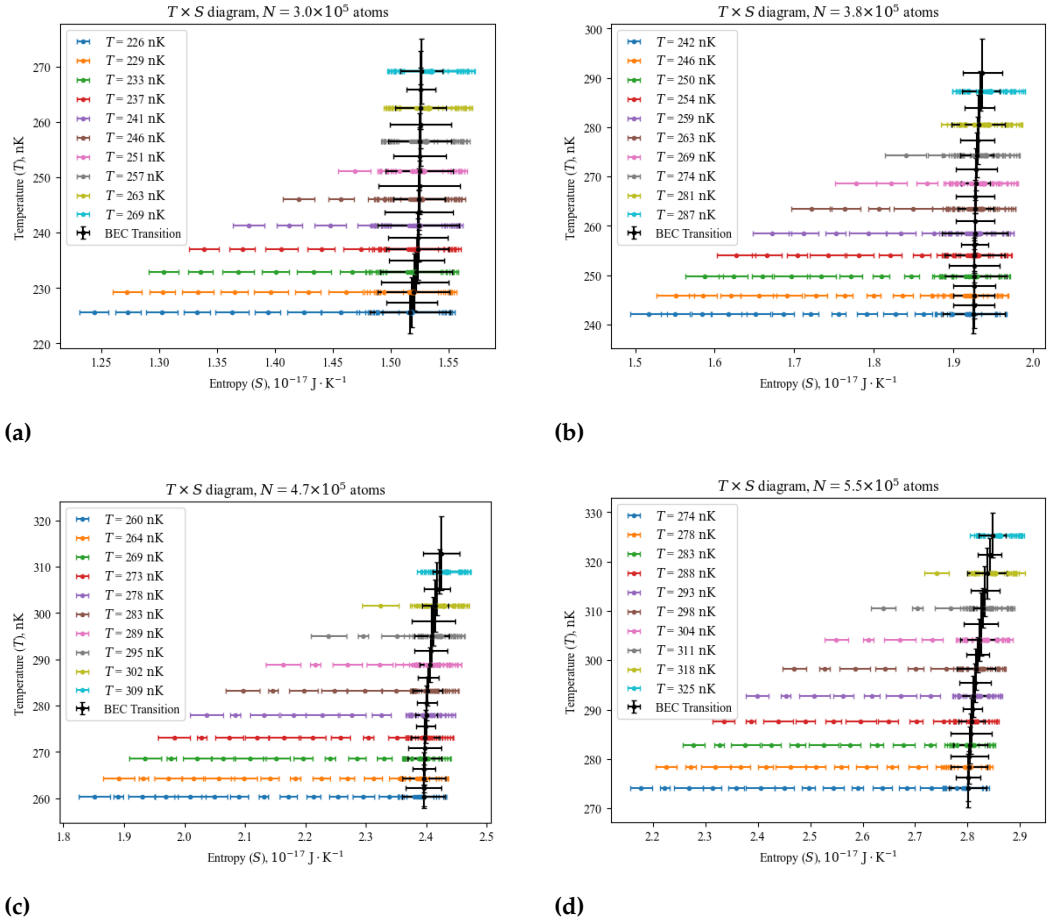

Figure 3. Selected temperature (T) versus entropy (S) diagrams.

To support the results in Fig. 3, let us demonstrate that the BEC transition is an isentropic process (S = constant) for an ideal gas (which was our basis for designing the empirical equation of state in Eq. (7) after all): since $U \cong 3\mathcal{P}\mathcal{V}$, from the internal energy in Eq. (2) we find at the BEC transition ($\mu = 0$) that

$$\mathcal{P} = \frac{(kT)^4}{\hbar^3} g_4(1). \tag{9}$$

Now, the non-Bose-condensed (thermal) atomic fraction of an ideal, harmonically trapped gas is well-known to be $N_T = N(T/T_c)^3$ for $T < T_c$, which may be written in the form $T = T_c(N_T/N)^{1/3}$. By raising that expression to the fourth power and substituting that and Eq. (1) into Eq. (9), we get

$$\mathcal{P} = \hbar \frac{g_4(1)}{g_3(1)} \left(\frac{N_T}{\mathcal{V}}\right)^{4/3} \quad \Longrightarrow \quad \mathcal{P}\left(\frac{\mathcal{V}}{N_T}\right)^{4/3} = \text{constant}. \tag{10}$$

At the BEC transition ($T = T_c$), $N_T \cong N$, which is constant, hence Eq. (10) becomes

$$\mathcal{P}\mathcal{V}^{3/4} = \text{constant at } T = T_c(\mathcal{V}). \tag{11}$$

Let us calculate the heat in a thermodynamic transformation from $(\mathcal{P}_1, \mathcal{V}_1)$ to $(\mathcal{P}_2, \mathcal{V}_2)$ over the level curve in Eq. (11), which represents the BEC transition. Since $U \cong 3\mathcal{P}\mathcal{V}$ and $\mathcal{P} = \text{const} \cdot \mathcal{V}^{-4/3}$, we have by the first law of thermodynamics that

 doi:10.20944/preprints202406.1225.v1

$$
\begin{aligned}
Q &= \Delta U + W = \Delta U + \int_{(\mathcal{P}_1,\mathcal{V}_1)}^{(\mathcal{P}_2,\mathcal{V}_2)} \mathcal{P}\mathrm{d}\mathcal{V} \\
&= (3\mathcal{P}_2\mathcal{V}_2 - 3\mathcal{P}_1\mathcal{V}_1) + \int_{(\mathcal{P}_1,\mathcal{V}_1)}^{(\mathcal{P}_2,\mathcal{V}_2)} \left(\frac{\text{const}}{\mathcal{V}^{4/3}}\right)\mathrm{d}\mathcal{V} \\
&= 3\cdot\text{const}\left(\frac{\mathcal{V}_2}{\mathcal{V}_2^{4/3}} - \frac{\mathcal{V}_1}{\mathcal{V}_1^{4/3}}\right) - 3\cdot\text{const}\cdot\frac{1}{\mathcal{V}^{1/3}}\Big|_{\mathcal{V}=\mathcal{V}_1}^{\mathcal{V}_2} \\
Q &= 0.
\end{aligned}
\tag{12}
$$

In conclusion, the BEC transition as a thermodynamic process is adiabatic. When that process is done in a reversible way, its entropy is also constant, which have already been shown by our experimental data in Fig. 3.

4.3. $T_cS_c \times N$ Diagram: Energy for Non-Mechanical Work

By grouping our experimental data at their constant values of $\mathcal{V}$, as they have been originally measured, we can determine the amount of energy available for non-mechanical work at BEC transition as the system's enthalpy, defined as $H = U + \mathcal{P}\mathcal{V}$, which from $U = TS - \mathcal{P}\mathrm{V}$ yields $H_c = T_cS_c$ at the transition. The curves of H_c versus N at selected values of $\mathcal{V}$ are seen in Fig. 4. For the operation of a generalized thermal engine, the product T_cS_c is more useful a quantity than the energy for mechanical work $\mathcal{P}\mathcal{V}$, which is "locked up" from use as the system's volume parameter is held constant.

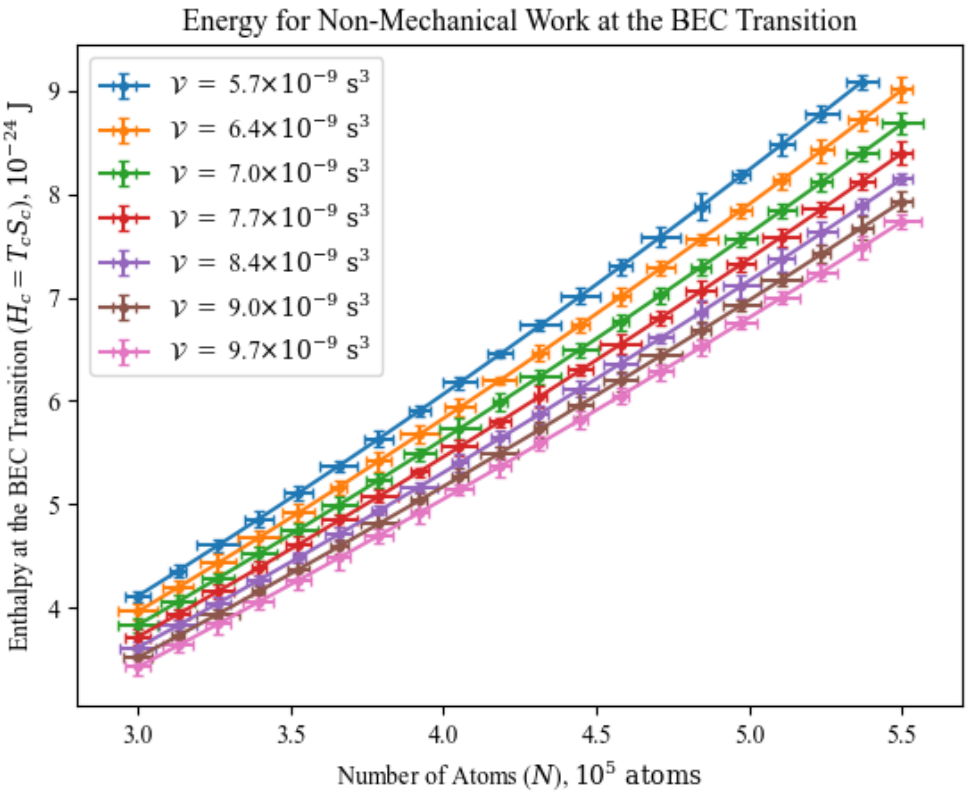

Figure 4. Constant volume parameter ($\mathcal{V}$) lines of enthalpy at the BEC transition ($H_c = T_cS_c$) versus the number of atoms (N). Since the BEC transition is isentropic, the enthalpy there represents the useful energy that can be drawn from it for doing non-mechanical work.

 doi:10.20944/preprints202406.1225.v1

Although the curves in Fig. 4 are not exactly straight lines, to due to the non-linear dependency of T_c with $\mathcal{V}$ that we observe even in Eqs. (3) and (5) for the ideal gas, it is clear that they can be approximated to a linear function, allowing us to gain insight into their behavior. Therefore, let us write a fitting line in the form

$$H_c = \eta N - H_c^0, \tag{13}$$

in which we call η the specific enthapic of transformation for BEC, and H_c^0 the intrinsic enthalpic loss. The former represents the energy per atom for cooling or heating the gas across the BEC transition at constant $\mathcal{V}$, i. e., without mechanical work. The latter is the amount of energy necessarily lost in adding zero to N atoms during the phase transition. We have fitted Eq. (13) to all constant $\mathcal{V}$ curves (including those not shown in Fig. 4), and the behavior of η and H_c^0 as functions of $\mathcal{V}$ is presented Fig. 5.

In Fig. 5a, there is a clear tendency of the specific enthalpy of transformation to decrease as the system's volume parameter increases, for the critical temperature decreases in that manner, as seen in Eqs. (3) and (5), all the while the entropy remains constant for all those values. In Fig. 5b, the enthalpic loss seems to remain constant as volume parameter varies, which indicates an intrinsic property of BEC. By drawing an analogy with chemistry, Eq. (13) can be seen as the variation of enthalpy of going from zero to N atoms collectively reaching temperature-density conditions for BEC.

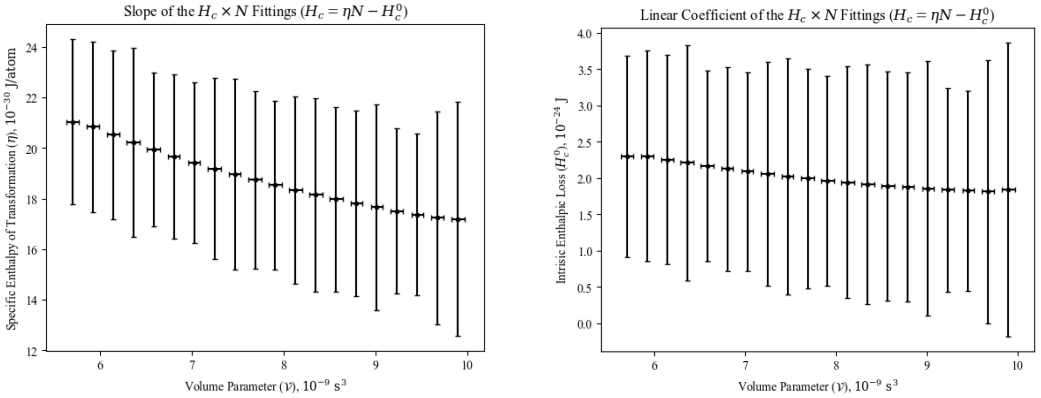

(a) Specific Enthalpy of Transformation **(b)** Intrinsic Enthalpic Loss

Figure 5. Results of fitting Eq. (13) to data in Fig. 4.

5. On Performing Thermodynamic Cycles on Quantum Gases

As we discussed in Secs. 3 and 4, experiments in our experimental setup are done at constant values of $\mathcal{V}$, which makes us turn our attention to the significance of non-mechanical work. In that scenario, it is possible to speculate about the potential implementation of thermodynamic cycles on gas samples under BEC, which consequently lead to idea of quantum thermal engines. For this analysis, we consider that the number of atoms N is held constant in all the possible processes described below.

- **Parametric-isochoric processes**: they follow the usual procedures mentioned in Sec. 3, with frequencies of the trapping potential measured and unchanged. In those cases, all the technical coefficients in Eq. (7) are constant, thus $\mathcal{P} = \mathcal{P}(T)$. By the mapping the currents on the coils that create the magnetic fields of the harmonic potential, it is possible to vary the volume parameter between each experimental sequence to produce a harmonically trapped gas sample.
- **Isothermal processes**: the steady state temperature of the gas sample in the harmonic trap is determined by its prior exposition to radiofrequency evaporation, which is a highly controllable and reproducible technique. Therefore, by mapping the exposition time and the strength of the radiofrequency signal, it is possible to achieve gas sample

 doi:10.20944/preprints202406.1225.v1

at the same temperature in different volume parameters. In that case, Eq. (7) becomes $\mathcal{P} = \mathcal{P}(\mathcal{V})$.

- **Parametric-isobaric processes**: from the equation of state in Eq. (7), one can determine the temperature values to obtain the same pressure parameter value at different volume parameters, with a combination of temperature and volume parameter from the two previously described processes. In those cases, the technical coefficients in Eq. (7) are varying together with the temperature, but in such a way that $\mathcal{P}(T, \mathcal{V}) = constant$ during the transformation.
- **Adiabatic processes**: by combining the first two processes described above, one can use Eq. (8) to find a set of temperature, volume parameter (and consequently pressure parameter) values that yield $S(T, \mathcal{V}) = constant$ throughout the transformation. A natural choice in those cases is the BEC transition, which have been shown to be an isetropic process in Fig. 3, whose critical temperature range can be estimated with the ideal gas' T_c in Eq. (5), adding the correction terms of the Hartree-Fock approximation [17] for a more precise estimation.

We remark that any thermodynamic cycle or process can be theoretically designed by exploiting Eqs. (7) and (8), and experimentally implemented by following the procedures listed above. One can determine the work performed during a cycle or process by calculating the area (for a cycle) or the path integral (for a process) it describes in a $\mathcal{P} \times \mathcal{V}$ diagram, as those seen in Fig. 2. The heat input and output of a cycle are found by calculating the path integrals of each process forming that cycle in a $T \times S$ diagram, as those in Fig. 3: the sum of positive results yields the heat input, and the sum of negative results yields the heat output. With those procedures, one can determine the efficiency of any cycle dividing its total work by its heat input. In this manner, we have a complete roadmap for implementing a thermal engine with a quantum gas.

6. Conclusions

We have presented here a full thermodynamic description of harmonically trapped gas samples with the Global-Variable Method in Secs. 4.1 and 4.2, which allow us to find all thermodynamic potentials of such a system, in contrast with the standard Local-Density Approximation (LDA) method. By designing an empirical expression for the equation of state in Eq. (7) and fitting it to significantly large dataset of measurements, we have been able to obtain entropy directly and find that its value is constant at the transition, confirming the known inexistence of latent heat for BEC.

Acknowledging that volume parameter is always constant in our measurements and in typical experiments with harmonic traps, thus prohibiting mechanical work, we determine the total energy available for non-mechanical work at the BEC transition by obtaining the system's enthalpy as a function of the number of atoms, for constant values of volume parameter, as shown in Fig. 4. Each constant volume parameter curve have been approximated by the linear function in Eq. (13), allowing us the achieve the specific enthalpy of transformation across the BEC transition, and the inherent enthalpic cost that is required of the system when temperature-density conditions for BEC are matched. To our knowledge, this is first time such informations is presented and discussed in the literature, showcasing the relevance of enthalpy for BEC.

We end our considerations by in delineating in Sec. 5 how the already established techniques for producing and imaging ultracold gas samples in harmonic traps can be used to perform thermodynamic cycles in operational laboratories across the world. In our perspective, this is the first approach into systematically building thermal engines with Bose-condensed gases, turning "quantum steampunk" into a physical reality.

Funding: This work was supported by the São Paulo Research Foundation (FAPESP) under the grant and 13/07276-1, and by the National Council for Scientific and Technological Development (CNPq) under the grant 2021/1008.

1. Mitchison, M.T. Quantum thermal absorption machines: refrigerators, engines and clocks. *Contemporary Physics* **2019**, *60*, 164–187.
2. Sur, S.; Ghosh, A. Quantum Advantage of Thermal Machines with Bose and Fermi Gases. *Entropy* **2023**, *25*, 372.
3. Koch, J.; Menon, K.; Cuestas, E.; Barbosa, S.; Lutz, E.; Fogarty, T.; Busch, T.; Widera, A. A quantum engine in the BEC–BCS crossover. *Nature* **2023**, *621*, 723–727.
4. Eglinton, J.; Pyhäranta, T.; Saito, K.; Brandner, K. Thermodynamic geometry of ideal quantum gases: a general framework and a geometric picture of BEC-enhanced heat engines. *New Journal of Physics* **2023**, *25*, 043014.
5. Estrada, J.A.; Mayo, F.; Roncaglia, A.J.; Mininni, P.D. Quantum engines with interacting Bose-Einstein condensates. *Physical Review A* **2024**, *109*, 012202.
6. Reyes-Ayala, I.; Miotti, M.; Hemmerling, M.; Dubessy, R.; Perrin, H.; Romero-Rochin, V.; Bagnato, V.S. Carnot Cycles in a Harmonically Confined Ultracold Gas across Bose–Einstein Condensation. *Entropy* **2023**, *25*, 311.
7. Miotti, M.P. Technical thermodynamics of an inhomogeneous gas around the Bose-Einstein transition using the global-variable method. PhD thesis, Universidade de São Paulo, 2021.
8. Romero-Rochín, V. Equation of state of an interacting Bose gas confined by a harmonic trap: The role of the "harmonic" pressure. *Physical review letters* **2005**, *94*, 130601.
9. Romero-Rochín, V.; Bagnato, V.S. Thermodynamics of an ideal gas of bosons harmonically trapped: equation of state and susceptibilities. *Brazilian journal of physics* **2005**, *35*, 607–613.
10. Romero-Rochín, V. Thermodynamics and phase transitions in a fluid confined by a harmonic trap. *The Journal of Physical Chemistry B* **2005**, *109*, 21364–21368.
11. Nascimbène, S.; Navon, N.; Jiang, K.; Chevy, F.; Salomon, C. Exploring the thermodynamics of a universal Fermi gas. *Nature* **2010**, *463*, 1057–1060.
12. Meyrath, T.; Schreck, F.; Hanssen, J.; Chuu, C.S.; Raizen, M. Bose-Einstein condensate in a box. *Physical Review A* **2005**, *71*, 041604.
13. Ketterle, W.; Durfee, D.S.; Stamper-Kurn, D. Making, probing and understanding Bose-Einstein condensates. *arXiv preprint cond-mat/9904034* **1999**.
14. Castin, Y.; Dum, R. Bose-Einstein condensates in time dependent traps. *Physical Review Letters* **1996**, *77*, 5315.
15. You, L.; Holland, M. Ballistic expansion of trapped thermal atoms. *Physical Review A* **1996**, *53*, R1.
16. De Groot, S.; Hooyman, G.; Ten Seldam, C. On the Bose-Einstein condensation. *Proceedings of the Royal Society of London. Series A. Mathematical and Physical Sciences* **1950**, *203*, 266–286.
17. Pethick, C.J.; Smith, H. *Bose–Einstein condensation in dilute gases*; Cambridge university press, 2008.